

## ADMITTANCE CHARACTERISTICS OF RADIAL AND THICKNESS VIBRATIONS OF THIN PIEZOCERAMIC DISKS

V. L. Karlash

**Experimental results on the forced radial and thickness vibrations of circular piezoceramic plates are analyzed. Experimental and theoretical amplitude–frequency plots for admittance and its active and reactive components are compared. It is established that the admittance–frequency characteristics are very dependent on the vibration mode and interelectrode capacitance. The calculations of admittance are in agreement with the experimental data.**

**Keywords:** piezoceramic circular resonator, admittance, impedance and phase shift, amplitude–frequency response

**Introduction.** In recent decades, piezoelectric plates of various geometry, primarily piezoceramic, have found wide application in vibration recording and controlling devices such as in sensors and actuators, as well as in multilayer metal-ceramic structures. Monolithic and composite piezoceramic plates with heterogeneous structure continue to be used in various types of piezoelectric transformers and frequency filters. Thin round plates are mainly used as microphones and telephones in mobile communications, as well as in piezofilters and current piezoelectric transformers.

Their major advantage over electromagnetic analogs is miniaturizability because their specific power can reach 20–40 W/in<sup>3</sup> [18]. The recent studies [7, 10, 18] show that the behavior of piezoelectric vibrators at high power strongly depends on the type of electric loading. The admittance–, conductance–, and susceptance–frequency responses at voltage of constant amplitude are essentially nonlinear, including abrupt drops and jumps, near resonance. Such nonlinearity is absent if the current is of constant amplitude [7, 18]. Study of the resonant electromechanical oscillations of piezoceramic plates is an important and urgent problem in the mechanics of coupled fields in materials and structural elements.

Radial and thickness vibrations of thin piezoceramic disks are monofrequency — overtones very far (by several time) in frequency from the principal resonances. The high intensity of radial oscillations and the pronounced dependence of their characteristic frequencies on Poisson's ratio allowed using radial oscillations to experimentally determine many important parameters of piezoceramics, such as planar EMCC  $k_p$ , transverse EMCC  $k_{31}$ , piezoelectric modulus  $d_{31}$ , Poisson's ratio  $\nu$ , elastic susceptibility components  $s_{11}$ ,  $s_{12}$ . The efficiency of electromechanical energy conversion in piezoelectric bodies is usually assessed in several ways: from the dynamic electromechanical coupling coefficient (EMCC) or from the full conductivity (admittance). There are no methods for the direct measurement of the active and reactive components of admittance; therefore, they have to be determined indirectly, i.e., calculated by various approximate formulas [1–7, 10].

This report presents analytical and experimental results on the admittance–frequency characteristics of the forced radial and thickness oscillations of a thin piezoceramic disk with continuous electrodes. The amplitudes and phases are calculated for the active and reactive components of the admittance. All calculations are made for complex quantities, taking into account dielectric, elastic, and piezoelectric losses [10–18]. The measurements were carried out using an advanced Mason circuit with an additional switch [9, 10].

In particular, it is shown that the amplitude–frequency characteristics of the admittance components depend on the vibration mode and the interelectrode capacitance of plate.

The calculated results are in good agreement with the experimental data.

**1. Admittance Components of Piezoceramic Disk Resonators.** A voltage  $U_{pe}$  applied to a piezoelectric element causes a current  $I_{pe}$ . The current/voltage ratio is, by definition, full conductivity or admittance  $Y$  [12–15]:

$$Y = \frac{I_{pe}}{U_{pe}}. \quad (1)$$

Since there are no amperemeters capable of measuring low currents at high frequencies, the current through a piezoelectric element is usually measured indirectly from the voltage drop across a special resistor connected in series [1, 5, 8, 10]. It is possible to easily show that the admittance of a piezoelectric element at any frequency results from the combination of the piezoelectric effect and static capacitance.

In [4], simple one-dimensional problems of electroelasticity were solved to obtain expressions for the input admittance of various piezoceramic vibrators such as rods with transverse and longitudinal polarization, thin circular disks and rings with thickness polarization, “short” and “high” cylindrical rings (shells), etc. As shown in [1, 14, 15], all they are reduced to the single complex formula

$$Y = j\omega C_0 \frac{\Delta_a(x)}{\Delta_r(x)}, \quad (2)$$

where  $j$  is imaginary unit;  $\omega$  is angular frequency;  $C_0$  is static capacitance;  $x$  is dimensionless frequency;  $\Delta_r(x)$  and  $\Delta_a(x)$  are resonant and antiresonant determinants.

Thus, the admittance  $Y$  of any piezoceramic vibrator at any frequency is the product of capacitive susceptance  $Y_C = j\omega C_0$  and the ratio of the antiresonant determinant to the resonant determinant.

The piezoelectric vibrators differ only in the complex expressions for the determinants  $\Delta_a(x)$  and  $\Delta_r(x)$ .

For thickness-polarized thin piezoceramic disks of radius  $R$  and thickness  $h$  with solid electrodes on the faces undergoing radial vibrations, the frequency determinants  $\Delta_r(x)$  and  $\Delta_a(x)$ , dimensionless complex frequency  $x$ , and squared planar electromechanical-coupling coefficient (EMCC)  $k_p^2$  are written as follows [4, 5, 15]:

$$\begin{aligned} \Delta_r(x) &= xJ_0(x) - (1-\nu)J_1(x), \\ \Delta_a(x) &= (1-k_p^2)\Delta(x) + (1+\nu)k_p^2J_1(x), \quad x = k^E R, \\ k^{E2} &= (1-\nu^2)\rho\omega^2 s_{11}^E, \quad x = x_0(1-0.5js_{11m}), \\ k_p^2 &= \frac{2d_{31}^2}{(1-\nu)s_{11}^E \varepsilon_{33}^T}, \quad d_{31}^2 = d_{310}^2(1-2jd_{31m}), \\ k_p^2 &= k_{p0}^2[1 + j(s_{11m} + \varepsilon_{33m} - 2d_{31m})], \quad C_{dsk} = C_{0dsk}(1 - j\varepsilon_{33m}), \quad C_{0dsk} = \frac{\varepsilon_{330}\pi R^2}{h}. \end{aligned} \quad (3)$$

Note that all the electroelastic coefficients in (2) and (3) as well as all the following expressions are complex [1, 2, 6, 10, 16]:

$$\begin{aligned} s_{11}^E &= s_{110}(1 - js_{11m}), \quad \varepsilon_{33}^T = \varepsilon_{330}(1 - j\varepsilon_{33m}), \quad d_{31} = d_{310}(1 - jd_{31m}), \\ s_{33}^E &= s_{330}(1 - js_{33m}), \quad d_{33} = d_{330}(1 - jd_{33m}), \end{aligned} \quad (4)$$

where the subscript “0” denotes the real part of a complex number, and the subscripts “m” denotes the ratio of imaginary part to real part, i.e., loss tangents [5, 10].

In the case of thickness oscillations of a thin piezoceramic disk, the expression for the frequency determinants  $\Delta_r(x)$  and  $\Delta_a(x)$  has the following form [4, 15]:

$$\begin{aligned}\Delta_{rt}(x_t) &= \cos(x_t), \\ \Delta_{at}(x_t) &= (1 - k_t^2) \Delta_t(x_t) + k_t^2 \sin x_t / x_t,\end{aligned}\quad (5)$$

and

$$\begin{aligned}C_{1t} &= C_{01t} (1 - j\varepsilon_{33m}), \quad x_t = x_{0t} (1 - 0.5js_{33m}), \\ C_{01t} &= \frac{\varepsilon_{330} \pi R^2}{h}, \quad x_t = k^t R, \\ k^{t2} &= \rho \omega^2 s_{33}^E, \quad k_t^2 = \frac{d_{33}^2}{s_{33}^E \varepsilon_{33}^T}, \\ d_{33}^2 &= d_{330}^2 (1 - 2jd_{33m}), \quad k_t^2 = k_{t0}^2 [1 + j(s_{33m} + \varepsilon_{33m} - 2d_{33m})].\end{aligned}\quad (6)$$

When calculating the admittance by formula (2) for a specific vibrator, the dimensionless,  $x_0$ , and measured,  $f_0$ , resonant frequencies are related by the formula

$$\omega C_0 = \frac{2\pi f_0 C_0 x}{x_0} = ax, \quad a = \frac{2\pi f_0 C_0}{x_0}, \quad (7)$$

where  $x$  is the current value of the dimensionless frequency.

**2. Experimental Technique, Amplitude–Frequency Characteristics.** The measurements were carried out using the advanced Mason circuit [1, 6, 9, 11] on several circular piezoceramic disks with solid silver electrodes on the faces made of PZT-19 or CTS TS-3 piezoceramics and polarized to thickness saturation. First, an E8-4 alternating-current bridge was used to measure the static capacitance  $C_0$  and loss tangent  $\tan \delta = e_{33m}$  at a frequency of 1000 Hz. Then, a matching voltage divider made of two series-connected resistors 68 and 10  $\Omega$  was connected to a G3-56/1 acoustic- and ultrasonic-frequency generator with an output resistance of 50  $\Omega$ . The tested piezoelectric elements with their pull-up resistors were connected through a switch in parallel to the output resistor of the divider. The frequency was measured with a Ch3-38 digital frequency meter, the voltage drop was measured with either a V2-27A/1 digital voltmeter or a V3-38 millivoltmeter. The thickness vibrations were studied using a G4-1A generator.

The voltage drops across the piezoresonator,  $U_{pe}$ , the load resistor  $U_R$ , and the input of the measurement circuit  $U_{in}$  were entered into the computer and used to compute the admittance  $Y_{pe}$  by formula (1). Its active,  $Y_{ac}$ , and reactive,  $Y_{re}$ , components were calculated using the phase shift between the voltage  $U_{pe}$  and the current  $I_{pe}$  or, which is the same, between the voltages  $U_{pe}$  and  $U_R$ :

$$\begin{aligned}Y &= Y_{pe} = \frac{I_{pe}}{U_{pe}} = \frac{U_R}{RU_{pe}}, \\ Y_{ac} &= Y_{pe} \cos \alpha, \quad Y_{re} = Y_{pe} \sin \alpha = Y_{pe} \sqrt{1 - \cos^2 \alpha}.\end{aligned}\quad (8)$$

The cosine of the phase shift angle was calculated by the cosine theorem [11–15]:

$$\cos \alpha = \frac{U_{pe}^2 + U_R^2 - U_{in}^2}{2U_{pe}U_R}. \quad (9)$$

The complex instantaneous power is the product between  $U_{pe}$  and  $I_{pe}$ :

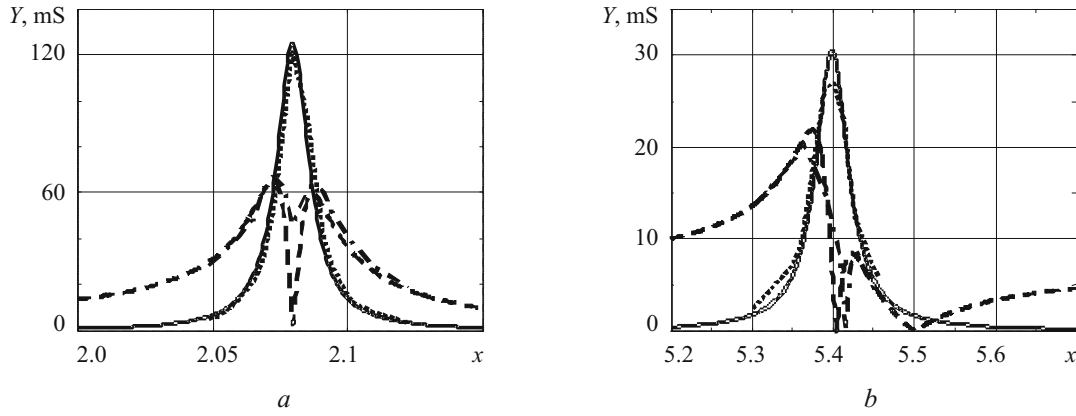


Fig. 1

$$P_{pe} = U_{pe} I_{pe} = \frac{U_R U_{pe}}{R}. \quad (10)$$

The advanced Mason circuit [1, 9] made it possible to carry out the measurements in several electric loading modes: given constant amplitude of one of the voltages  $U_{in}$ ,  $U_{pe}$  or  $U_R$ , and “as is” conditions where these voltages are arbitrary and the ratios between them are set automatically. The fact is that, in the presence of a matching divider in the measurement circuit, the voltage drop  $U_{in}$  at its output does not remain constant during frequency tuning, but constantly varies due to the shunting effect of the piezoresonator. The author has developed a technique that allows, based on the data obtained “as is,” to study the effect of other electrical loading modes on the characteristics of the specimens [13].

For the first radial resonance of the forced electromechanical oscillations of the TsTBS-3 piezoceramic disk with a diameter of 66.1 mm and a thickness of 3.1 mm the following values were obtained:  $C_0 = 18490$  pF,  $\tan \delta = 0.0066$ ,  $a = 1,77$  mC,  $\nu = 0.35$ ,  $k_p^2 = 0.3$ ,  $s_{11m} = 0.0069$ ,  $\varepsilon_{33m} = 0.0085$ ,  $d_{31m} = 0.0076$ ,  $x_{01} = 2.08$ ,  $f_{01} = 31.59$  kHz. Figure 1a shows for the absolute values of the active and reactive components of the input admittance in the dimensionless frequency range  $2.00 \leq x \leq 2.15$ . To plot the theoretical and experimental curves in the same figures, the following comparison formula [15] was used:

$$x_0 = xx_{01} / f_{01}. \quad (11)$$

Here  $x$  is the current value of the dimensionless frequency;  $x_{01}$  and  $f_{01}$  are the dimensionless and measured frequencies of the admittance peaks.

Note that the values taken for the calculation of  $k_p^2$ ,  $s_{11m}$ ,  $\varepsilon_{33m}$ ,  $d_{31m}$  and  $k_t^2$ ,  $s_{33m}$ ,  $\varepsilon_{33m}$ ,  $d_{33m}$  for thickness oscillations (see below) were obtained by successive iterations based on the author’s iteration technique developed before [2, 10, 12]. The measurements were carried out for a pull-up resistor of  $11.2 \Omega$  in the “as is” mode. Absolute values are taken because the voltmeter measures voltage irrespective of its polarity.

The theoretical and experimental graphs for the conductance are represented by solid and dashed lines, respectively. The theoretical and experimental graphs for the susceptance are represented by dashed and dot–dash lines, respectively.

The conductances are in very good agreement, whereas the susceptances differ substantially near zero. This difference may be due to the insufficient number of data points near the maximum or the inaccurate value of  $k_p^2$  chosen.

Figure 2b represents the second radial resonance of the same disk in the dimensionless frequency range  $5.2 \leq x \leq 5.7$  for  $x_{01} = 5.4$ ,  $f_{02} = 83.1$  kHz, and  $s_{11m} = 0.009$ . The other values are the same as for the first radial resonance. The conductances are in good agreement, while the susceptances slightly differ at zero, but have similar slopes. The cause of the more noticeable difference can be the insufficient number of data points near the maximum of the active component or the different degree of high-frequency “squeezing” of the piezoelectric element’s capacitance in the principal radial mode and at its overtones.

In the case of thickness oscillations of the disk, calculations were carried out using formulas (2), (5)–(7) and the following data:  $k_t^2 = 0.3$ ,  $s_{33m} = 0.021$ ,  $\varepsilon_{33m} = 0.01$ ,  $d_{33m} = 0.01$ ,  $a_t = 30$  mS,  $f_{0t} = 650$  kHz.

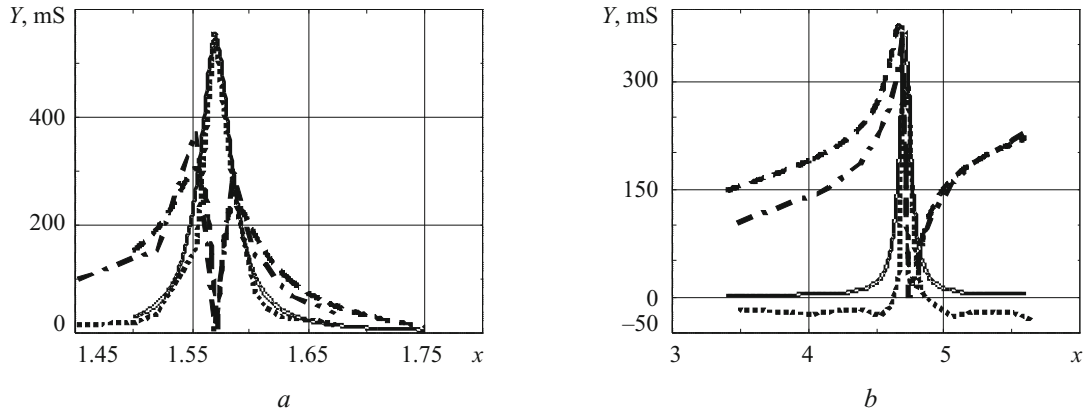


Fig. 2

Figure 2a is plotted for dimensionless frequency range  $1.45 \leq x \leq 1.75$  using the formula  $x_0 = x \cdot 1.57/650$ . The curve notation is the same as in Fig. 1. The curves in Fig. 2b are plotted for the first overtone of thickness oscillations, i.e., for the frequency range  $3.4 \leq x \leq 5.6$ . Now:  $k_t^2 = 0.3$ ,  $s_{33m} = 0.021$ ,  $\epsilon_{33m} = 0.01$ ,  $d_{33m} = 0.01$ ,  $a_t = 60$  mS,  $f_{0t} = 2160$  kHz,  $x_0 = x \cdot 4.71/2160$ .

At a high frequency, the “squeezing” of the capacitance of the specimen is very noticeable, as evidenced by the magnitude of the factor  $a_t$ . In order to match the measured value of the active component of the total conductivity with the calculated value, this parameter had to be increased not thrice, but only twice. In this case, the calculated and experimental graphs are similar in form.

**3. Experimental Data Analysis, Admittance Circles.** If the magnitude of the active component  $G$  of admittance is plotted along the abscissa, and the reactive component  $B$  is plotted along the ordinate, then we obtain the so-called admittance circle [4, 5]. Figure 3 shows the calculated (solid lines) and experimental (dashed lines) admittance circles for the first two radial and first two thickness modes of the piezoceramic disk (graphs in Fig. 3a, b, c, and d, respectively). Since the voltmeters used to measure the voltage drops do not respond to the polarity of the measured voltage, we had to put the magnitudes of the quantities along the vertical axis. This resulted in two semicircles, one under the other. These “semicircles” for the disk under consideration, do not always coincide with each other because of the effect of the interelectrode capacitance.

Comparison of the calculated and experimental graphs shows that the general trends of the curves (with frequency) agree well. As in Figs. 2 and 3, differences are observed near “zero” of the reactive components; at the same frequencies, the admittances and their active components reach the maximum. In the author’s opinion, the cause of the differences is the following. Due to the high mechanical quality factor of the resonator ( $Q_{mr} = 1/s_{11m} = 1/0.0069 = 144.9$  in the principal radial mode and  $Q_{mt} = 1/s_{33m} = 1/0.021 = 47.8$  in the first thickness mode), it is very difficult to manually adjust the frequency of the generators at these points. The fact is that abrupt changes in electrical voltage occur in a frequency range of only a few dozens of hertz.

All graphs clearly show a significant effect of the static capacitance  $C_0$  of the piezodisk. The higher the frequency, the higher the effect. The first harmonic resonance frequency of the thickness oscillations of 2160 kHz exceeds the resonant frequency of the principal radial resonance of 31.59 kHz by almost 70 times, and the influence of the capacitive component of the input admittance is so high that the graphs are completely located in the region of positive values of the reactive component, giving rise to a full circle of admittance (see Fig. 3d).

**Conclusions.** Based on the study, we can draw the following conclusions.

1. The conductance– and susceptance–frequency responses are similar for all oscillation modes of piezoelectric vibrators, though their amplitudes differ by a factor of almost 20, from 20 mS (at the first overtone of radial oscillations) to 560 mS (in the principal thickness mode). The frequency of the first overtone of the thickness oscillations exceeds the resonant frequency of the fundamental radial mode by many dozen times.

2. It is easy to see that for comparing the experimental results with the calculation, the admittance circles (in this case, semicircles) are very illustrative, but it is difficult to plot the characteristic frequencies on them. On the other hand, the frequency response is well illustrated by frequency dependences, but they are not so illustrative. In the author’s opinion, it is convenient to study the admittance characteristics of piezoceramic resonators when comparing graphs, as done in this article.

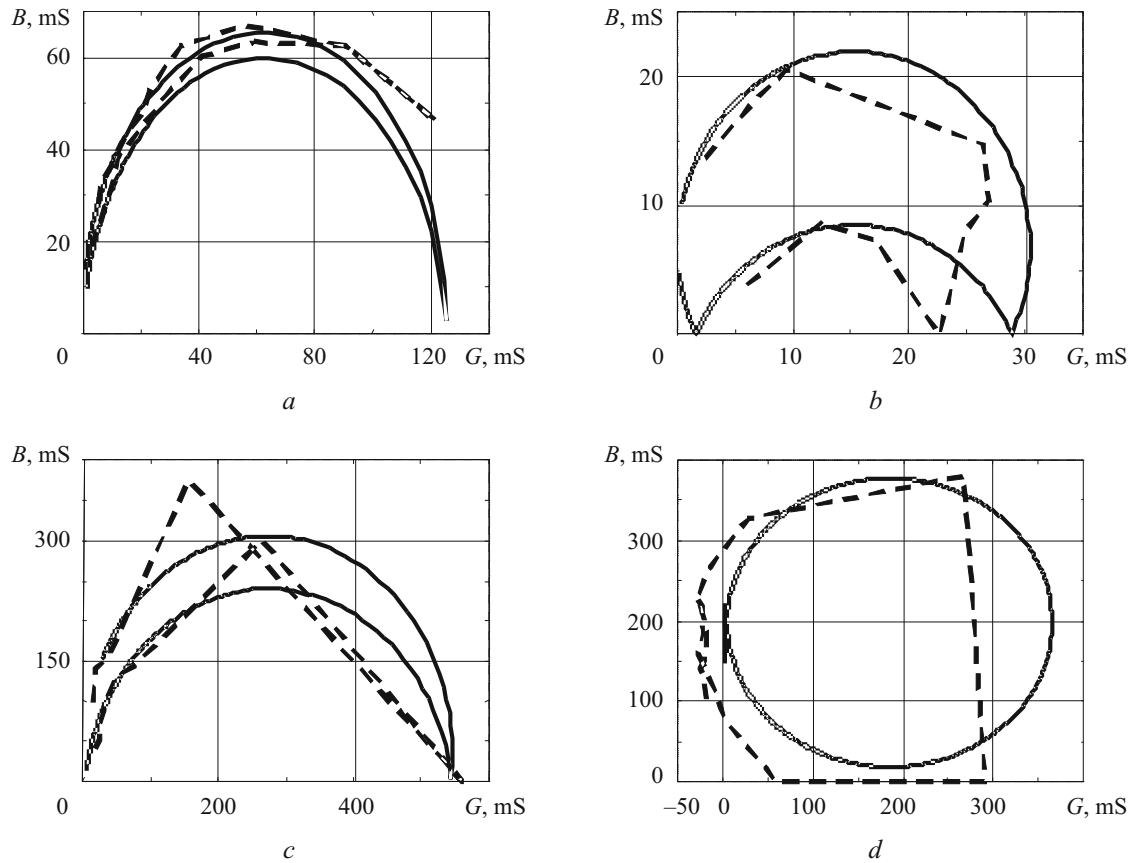


Fig. 3

3. The amplitude–frequency characteristics of the active and reactive components of admittance strongly depend on the vibrational mode and the interelectrode capacitance, the effect of which is the stronger, the higher the oscillation frequency is.

The basic shortcoming of the author’s methods [1–3, 11–15] is that they neglect the frequency–dependence of the dielectric losses, which are independently measured at a frequency of 1000 Hz. This shortcoming has a weak effect on the operation of piezoelectric vibrators at frequencies up to several tens of kilohertz, yet can become strong in the megahertz range.

## REFERENCES

1. V. L. Karlash, “Methods for determining the coupling coefficients and energy loss in vibrations of piezoceramic resonators,” *Akust. Visn.*, **15**, No. 4, 24–38 (2012).
2. V. L. Karlash, “Revisiting the loss of energy in piezoceramic resonators,” *Akust. Visn.*, **17**, No. 1, 34–47 (2015).
3. V. L. Karlash, “Comparison of experimental and calculated data in the study of forced oscillations of piezoceramic resonators,” *Akust. Visn.*, **17**, No. 3, 13–20 (2015).
4. N. A. Shul’ga and A. M. Bolkisev, *Oscillations of Piezoelectric Bodies* [in Ukrainian], Naukova Dumka, Kyiv (1990).
5. M. O. Shul’ga and V. L. Karlash, *Resonance Electromechanical Oscillations of Piezoelectric Plates* [in Ukrainian], Naukova Dumka, Kyiv (2008).
6. M. O. Shul’ga and V. L. Karlash, “Amplitude–phase characteristics of radial oscillations of a thin piezoceramic disk near resonances,” *Dop. NAN Ukrainy*, No. 9, 80–86 (2013).
7. O. I. Bezverkhyy, L. P. Zinchuk, and V. L. Karlash, “Modelling of the piezoceramic resonator electric loading conditions based on experimental data,” *Math. Model. Comput.*, **2**, No. 2, 115–127 (2015).
8. “IRE standards on piezoelectric crystals: Measurements of piezoelectric ceramics,” *Proc. IRE*, **49**, 1161–1169 (1961).

9. V. L. Karlash, "Particularities of amplitude–frequency characteristics of admittance of thin piezoceramic half-disk," *Int. Appl. Mech.*, **45**, No. 10, 647–653 (2009).
10. V. L. Karlash, "Energy losses in piezoceramic resonators and its influence on vibrations' characteristics," *Electronics and Communication*, **19**, No. 2, 82–94 (2014).
11. V. L. Karlash, "Modeling of energy-loss piezoceramic resonators by electric equivalent networks with passive elements," *Math. Model. Comput.*, **1**, No. 2, 163–177 (2014).
12. V. L. Karlash, "Analysis of the methods of determination of the viscoelastic coefficients of piezoceramic resonators," *J. Math. Sci.*, **226**, No. 2, 123–138 (2017).
13. V. L. Karlash, "Influence of electric loading conditions on the vibrations piezoceramic resonators," *Int. Appl. Mech.*, **53**, No. 2, 220–227 (2017).
14. V. L. Karlash, "Phase–frequency characteristics of the longitudinal and transverse vibrations of planar piezoceramic transformers," *Int. Appl. Mech.*, **53**, No. 3, 349–355 (2017).
15. V. L. Karlash, "Conductance– and susceptance–frequency responses of piezoceramic vibrators," *Int. Appl. Mech.*, **53**, No. 4, 464–471 (2017).
16. G. Liu, S. Zhang, W. Jiang, and W. Cao, "Losses in ferroelectric materials," *Mater. Sci. Eng. Reports*, **89**, 1–48 (2015).
17. A. V. Mezheritsky, "Elastic, dielectric and piezoelectric losses in piezoceramics; how it works all together," *IEEE Trans. UFFC*, **51**, No. 6, 695–797 (2004).
18. K. Uchino, Yu. Zhuang, and S. O. Ural, "Loss determination methodology for a piezoelectric ceramic: new phenomenological theory and experimental proposals," *J. Adv. Dielectric*, **1**, No. 1, 17–31 (2011).